PHYSOR 2004 - the Physics of Fuel Cycles and Advanced Nuclear Systems: Global Developments
Chicago, Illinois, April 25-29, 2004, on CD-ROM, American Nuclear Society, Lagrange Park, IL. (2004)

3D Characteristics Method with Linearly Anisotropic Scattering

M. Dahmani[1], R. Roy and J. Koclas
Nuclear Engineering Institute, École Polytechnique de Montréal
P.O.BOX 6079, Station Centre-ville, Montréal, Québec, Canada H3C 3A7

The objective of this work is to extend the characteristics method to take into account anisotropic scattering effects in 3D geometries. Only the linearly anisotropic scattering cross sections and sources treatment will be considered.
The method of characteristics is based on computing the angular flux following the tracking lines. Therefore, the implementation of anisotropic sources is relatively simpler than in collision probability method. However, the calculation of the anisotropic sources requires large amount of memory in order to store the angular flux per energy group, region, direction and track. Comparisons between the isotropic and anisotropic fluxes for different meshing and number of discretized angles will be shown in the results section.

KEYWORDS: Characteristics method, anisotropic, scattering.

1. Introduction

The recent advances in computer capability in term of memory size and processor speed, on one hand, and the development of high performance computing methods on the other hand allow investigating the boundaries of the old models in many scientific and engineering applications. Like other applications, the advanced reactor core designs require advanced computational methods in order to achieve high accuracy in reasonable computational time. To assure this accuracy, in advanced reactor core analysis methods based on transport equation solution using the deterministic transport codes, the approximations used must be reviewed to take into account of:

- Space: the 3D geometry configuration with great degree of heterogeneity;
- Energy: to enlarge by refining the discritization of the domain to treat well the resonance regions;
- Angle: to allow the use of the large number of discrete angles to eliminate in part the ray effects and to treat the anisotropic effects.

[1]Corresponding author: E-mail: mohamed.dahmani@polymtl.ca, Fax: 514-340-4192

In this paper, we present the extension of the 3D characteristics method to take into account the anisotropic effects. We will limit our analysis to the linearly anisotropic scattering cross sections and sources. The anisotropic treatment has been presented in several papers for 2D geometries using the Collision Probabilities method [1-3] and Method of Characteristics. [4,5]

Since MOC is based on computing the angular flux on tracks, the implementation of the anisotropic sources is relatively simpler than in CP. However, the calculation of the anisotropic sources requires large amount of memory in order to store the angular flux per energy group, region, direction and track. This implementation is done in the 3D Characteristics solver [6], a part of DRAGON code. [7] The comparison between the isotropic and anisotropic fluxes for different meshing and number of discretized angles will be shown in the results section.

The ramainder of this paper is organized as follows. In section 2 we derive the characteristics equations using the linearly anisotropic scattering. The discretized characteristics equations are also presented in this context. In section 3 we describe the calculation methodology and the algorithm used. Finally numerical results comparing the isotropic and anisotropic fluxes will be shown.

2. Characteristics Equation with Anisotropic Scattering

The multigroup transport equation to be solved to obtain the flux from a source Q is:

$$B^g(\vec{r},\hat{\Omega})\Phi^g(\vec{r},\hat{\Omega}) = Q^g(\vec{r},\hat{\Omega}) \tag{1}$$

where:

- $\vec{r}$ is a spatial point in the domain D;
- $\hat{\Omega}$ is the solid angle;
- g is the energy group;
- $B^g(\vec{r},\hat{\Omega}) = \hat{\Omega}\cdot\vec{\nabla} + \Sigma^g(\vec{r})$ is the transport operator in group g;
- $\Sigma^g(\vec{r})$ is the total cross section in group g;
- $Q^g(\vec{r},\hat{\Omega})$ is the anisotropic source in group g.

The source in Eq.(1) is composed of two terms, the fission and scattering sources:

$$Q^g(\vec{r},\hat{\Omega}) = F^g(\vec{r}) + S^g(\vec{r},\hat{\Omega}) \tag{2}$$

The isotropic fission source is given by:

$$F^g(\vec{r}) = \frac{\chi^g}{4\pi\, K_{\text{eff}}}\sum_{g'} \nu\,\Sigma_f^{g'}(\vec{r})\phi^{g'}(\vec{r}) \tag{3}$$

where $\phi^{g'}(\vec{r})$ is the scalar flux in group g.

Using the first order Legendre polynomial expansion on angular flux and scattering cross section, the linear anisotropic scattering source is obtained by:

$$S^g(\vec{r},\hat{\Omega}) = S_0^g(\vec{r}) + S_1^g(\vec{r},\hat{\Omega}) \tag{4}$$

where:

$$S_0^g(\vec{r}) = \frac{1}{4\pi}\sum_{g'} \Sigma_{s0}^{g\leftarrow g'}(\vec{r})\phi^{g'}(\vec{r}) \tag{5}$$

is the isotropic scattering source. The anisotropic scattering source term is given by:

$$S_1^g(\vec{r},\hat{\Omega}) = \frac{3}{4\pi}\sum_{g'} \Sigma_{s1}^{g\leftarrow g'}(\vec{r}) \int_{4\pi} d^2\Omega' \; \hat{\Omega}.\hat{\Omega}'\Phi^{g'}(\vec{r},\hat{\Omega}') \tag{6}$$

The main idea behind the characteristics method is to solve the differential form of the transport equation following the straight lines (characteristics or tracking lines). The neutron trajectories will be followed in the local coordinates system where an observer is traveling in the neutron direction. The basic transport operator is transformed into a total differential operator:

$$B^g(\vec{r},\hat{\Omega}) \rightarrow C^g(s) = \frac{d}{ds} + \Sigma^g(\vec{r}+s\hat{\Omega}), \tag{7}$$

where: $C^g(s)$ is the characteristics operator in group g, s is the variable along a line. The multi-group characteristics equation is then given by:

$$C^g(s)\Phi^g(\vec{r}+s\hat{\Omega}) = Q^g(\vec{r}+s\hat{\Omega},\hat{\Omega}). \tag{8}$$

The average scalar flux in region j with volume equal to V_j and in group g is obtained by integrating over volume and directions:

$$\begin{aligned} V_j\Phi_j^g &= \int_{V_j} d^3r \int_{4\pi} d^2\Omega \; \Phi^g(\vec{r},\hat{\Omega}) \\ &= \int_{\Upsilon} d^4T \int_{-\infty}^{+\infty} dt \; \chi_{V_j}(\vec{T},t) \; \Phi^g(\vec{p}+t\hat{\Omega},\hat{\Omega}). \end{aligned} \tag{9}$$

A characteristics line $\vec{T}$ is determined by its orientation $\hat{\Omega}$ along with a reference starting point $\vec{p}$ for the line. Variable t refers to the local coordinates on the tracking line, and the function $\chi_{V_j}(\vec{T},t)$ is defined as 1 if the point $\vec{p}+t\hat{\Omega}$ on the line $\vec{T}(\hat{\Omega},\vec{p})$ in the region V_j, and 0 otherwise. The d^4T element is then decomposed into a solid angle element $d^2\hat{\Omega}$ and a corresponding plane element d^2p which constitute the Υ domain.

2.1 Discretization of Characteristics Equations

The spatial and the angular domains are sampled using a ray tracing procedure as described in [6]. The Υ domain is first covered by choosing a quadrature set of solid angles, composed of discretized directions and their corresponding weights $(\hat{\Omega}_i,\omega_i)$. We generally use the Equal Weight Quadrature (EQ_N) to generate the angular directions.[9] Then, the plane $\Pi_{\hat{\Omega}_i}$ perpendicular to any selected direction i, is split into a Cartesian grid meshing and the starting points

$\vec{p}_{i,n}$ of each characteristics are found. For each discretized direction i, a whole set of tracks $\vec{T}_{i,n}$ will be generated. When travelling across different regions, the neutron beam following the characteristics crosses $K_{i,n}$ segments numbered by index k; the segment lengths are labeled $L_{i,n,k}$ and the region numbers are N_k. The multigroup discretized equations are then derived from Eq. 8 as:

$$\frac{d}{ds_{j,i,n,k}}\Phi^g_{j,i,n,k} + \Sigma^g_j \Phi^g_{j,i,n,k} = F^g_j + S^g_{0,j} + S^g_{1,j,i,n,k} \tag{10}$$

The anisotropic source is obtained from the discretization of Eq. 6:

$$S^g_{1,j,i,n,k} = \frac{3}{4\pi}\sum_{g'} \Sigma^{g\leftarrow g'}_{s1,j} \sum_m \omega_m \left(\hat{\Omega}_i.\hat{\Omega}_m\right) \Phi^g_{j,m,n,k} \tag{11}$$

where ω_m are the angular weights in the quadrature and the solid angle vector is given by:

$$\hat{\Omega}_i \equiv \begin{bmatrix} \sqrt{1-\mu_i^2}\cos\varphi_i \\ \sqrt{1-\mu_i^2}\sin\varphi_i \\ \mu_i = \cos\theta_i \end{bmatrix} \equiv \begin{bmatrix} \cos\gamma_i \\ \cos\lambda_i \\ \mu_i = \cos\theta_i \end{bmatrix} \tag{12}$$

where $\cos\gamma_i$, $\cos\lambda_i$, μ_i are the director cosines on x, y and z axis respectively. Using the relationship between these two angles representations, we obtain:

$$\begin{cases} \Theta_{i,m}(\mu,\varphi) = \mu_i\mu_m + \sqrt{1-\mu_i^2}\sqrt{1-\mu_m^2}\cos(\varphi_i - \varphi_m) = \Theta_{i,m}(\mu,\gamma,\lambda); \\ \varphi_i = Arctan\left(\frac{\cos\lambda_i}{\cos\gamma_i}\right); \\ S^g_{1,j,i,n,k} = \frac{3}{4\pi}\sum_{g'}\Sigma^{g'}_{s1,j}\sum_m \omega_m \Theta_{i,m}(\mu,\gamma,\lambda)\Phi^g_{j,m,n,k}. \end{cases} \tag{13}$$

Assume that the segment k crosses region j, then the local relationship between the incoming and outgoing angular flux is given by integrating the Eq. 10 along the track:

$$^{\text{out}}\phi^g_{j,i,n,k} = {}^{\text{in}}\phi^g_{j,i,n,k} + \left[\frac{\tilde{Q}^g_j}{\Sigma^g_j} + \frac{S^g_{1,j,i,n,k}}{\Sigma^g_j} - {}^{\text{in}}\phi^g_{j,i,n,k}\right] E(\tau^g_{j,i,n,k}) \tag{14}$$

where:

$^{\text{out}}\phi^g_{j,i,n,k} = \phi^g_{j,i,n,k}(L_{i,n,k});$

$^{\text{in}}\phi^g_{j,i,n,k} = \phi^g_{j,i,n,k}(0);$

$\tau^g_{j,i,n,k} = \Sigma^g_j L_{i,n,k}$, is the neutron optical path;

$E(x) = 1 - e^{-x}$.

$\tilde{Q}^g_j$ is composed of fission and isotropic scattering sources. We then integrate Eq. 14 along the segment to get the segment average angular flux. Assuming that the track lengths have been normalized to ensure volume conservation, the average angular flux per region is given by:

$$\Sigma^g_j V_j \bar{\Phi}^g_{j,i} = V_j\tilde{Q}^g_j + \sum_{nls}\pi_{i,n}\sum_k \delta_{jN_k}\left[S^g_{1,j,i,n,k}L_{i,n,k} + \Delta^g_{j,i,n,k}\right] \tag{15}$$

where $\Delta^g_{j,i,n,k} = {}^{\text{in}}\phi^g_{j,i,n,k} - {}^{\text{out}}\phi^g_{j,i,n,k}$ is the flux difference on segment k and $\pi_{i,n}$ is the weight associated with track $\vec{T}_{i,n}$.

The average scalar flux in region j and energy group g is computed by integrating Eq. (15) over all directions to obtain:

$$\phi_j^g \;=\; \frac{\tilde{Q}_j^g}{\Sigma_j^g} + \frac{1}{\Sigma_j^g V_j} \sum_i \omega_i \sum_n \pi_{i,n} \sum_k \delta_{jN_k} \left[S_{1,j,i,n,k}^g L_{i,n,k} + \Delta_{j,i,n,k}^g \right] \tag{16}$$

From this equation, we see that the iteration sweep over all characteristics involves the sequential evaluation of outgoing fluxes of Eq.(14) on every single track and the adding of flux differences $\Delta_{j,i,n,k}^g$ for each track $\vec{T}_{i,n}$ in Eq.(16).

2.2 Boundary Conditions

At the boundary of the external surfaces, the outgoing current is calculated using the angular flux computed on the segment K crossing the surface α:

$$J_\alpha^+ = \sum_i \omega_i \sum_n \pi_{i,n} \chi_{\alpha,K} \hat{\Omega}_i \cdot \hat{N}_\alpha \; {}^{\text{out}}\phi_{j,i,n,K}, \quad \hat{\Omega}_i \cdot \hat{N}_\alpha > 0 \tag{17}$$

and $\chi_{\alpha,K}$ is defined as:

$$\chi_{\alpha,K} = \begin{cases} 1, if\ \vec{r} \in S_\alpha \\ \\ 0, otherwise. \end{cases} \tag{18}$$

The current is composed of two terms:

$$J_\alpha^+ = {}^{\text{iso}}J_\alpha^+ + {}^{\text{aniso}}J_\alpha^+ \tag{19}$$

where:

$${}^{\text{iso}}J_\alpha^+ = \sum_i \omega_i \sum_n \pi_{i,n} \chi_{\alpha,K} \hat{\Omega}_i \cdot \hat{N}_\alpha \left[{}^{\text{in}}\phi_{j,i,n,K} + \left(\frac{\tilde{Q}_j}{\Sigma_j} - {}^{\text{in}}\phi_{j,i,n,K} \right) E(\tau_{j,i,n,K}) \right] \tag{20}$$

is the isotropic part of the current ($S_1 = 0$) and

$${}^{\text{aniso}}J_\alpha^+ = \sum_i \omega_i \sum_n \pi_{i,n} \chi_{\alpha,K} \hat{\Omega}_i \cdot \hat{N}_\alpha \left(\frac{S_{1,j,i,n,K}}{\Sigma_j} E(\tau_{j,i,n,K}) \right) \tag{21}$$

is the anisotropic part. We apply then the quasi-isotropic reflection with albedo. The reflected neutrons are entering at the same position on surfaces but in the opposite directions:

$$J_\alpha^- = \beta_\alpha J_\alpha^+ \tag{22}$$

3. Calculation Methodology and Implementation

In order to compute the anisotropic sources, using the Eq. 13, we must store the angular flux per energy group, region and direction. Therefore, two characteristics sweeps are necessary:

1. compute and store the angular flux per energy group, region and direction;
2. compute the anisotropic scattering source.

This two steps are implemented at the inner iteration procedure. Consequently, the convergence takes more CPU time than without anisotropic scattering sources and the memory size needed is also very large. The global computational scheme is described in the next subsection.

3.1 Computational scheme

initialisation: currents and fluxes.

1. Guess new fission sources and incoming current (**outer loop**);
   (a) Guess scattering sources (**inner loop**);
   (b) Compute the flux for each energy group:
      i. *First characteristics sweep*: compute and store the angular flux per energy group, region, direction;
      ii. *Second characteristics sweep*: compute the anisotropic scattering source;
      iii. compute the outgoing current at the boundary surfaces and apply the boundary conditions;
      iv. compute the scalar flux.
   (c) apply global inner acceleration technique.
   (d) If flux map are not converged, go to (a).
2. Apply global outer acceleration techniques;
3. Compute the K_{eff} for next neutron generation;
4. If not converged, go to 1.

4. Numerical results

The 3D problem we treat here is the extension of the 2D Lathrop one group problem described in [4]. The geometry of the problem is a $[0,2] \times [0,2] \times [0,2]$ centimeter cube with a fixed source located in $[0,1] \times [0,1] \times [0,1]$ cube. The total and isotropic scattering cross-sections are $\Sigma_t = 0.75\ cm^{-1}$ and $\Sigma_{s0} = 0.5\ cm^{-1}$ respectively. For the anisotropic problem, we add a forward-scattering cross-section $\Sigma_{s1} = 0.5\ cm^{-1}$ everywhere. Reflections are assumed as boundary conditions on all faces. Our analysis is based on the comparison between the isotropic and the anisotropic solutions. To do so, two different metrics are used:

$$E_{max} = \max_j \left(\frac{\mid \phi_j^{aniso} - \phi_j^{iso} \mid}{\phi_j^{iso}} \right) \times 100; \qquad (23)$$

and

Table 1: Maximum percentage error for different spatial splitting

Meshing	E_{max}(%)
$2{\times}2 \times 2$	12.69
$4{\times}4 \times 4$	17.99
$8{\times}8 \times 8$	18.47

Table 2: CPU time for the two solutions

Solution	Isotropic	Anisotropic
CPU Time (s)	59	1630
Number of iterations	13	13

$$E_j = \frac{\mid \phi_j^{aniso} - \phi_j^{iso} \mid}{\phi_j^{iso}} \times 100; \tag{24}$$

where E_{max} and E_j are the maximum percentage error on all regions and the percentage error for a given region respectively.
ϕ_j^{aniso} and ϕ_j^{iso} are the anisotropic and isotropic integrated flux in region j respectively.
The Equal Weight Quadrature EQ_N [9] is used to discretize the angular variable, the number of angles is given by:

$$Nang = \frac{N(N+2)}{8} \tag{25}$$

We use different meshing by splitting the domain on equivolumetric zones, different number of angles by varing the values of N in the quadrature and different density of tracks (DT). In Table 1, we show the maximum errors for different meshing. We use 8 angles and a density of tracks equal to 20 tracks/cm^2. It shows that the max error varies slightly with the spatial meshing. However, the max error on fluxes reaches about 18%.
We have fixed the values of x and y at $0.25cm$ respectively and then we present the values of the scalar flux, with and without anisotropic scattering, corresponding to different z-planes. the percent errors between the two fluxes is important in the first four z-planes where the external source is located Fig. 1. The anisotropic scalar flux map is also shown in Fig. 2. We observed that the highest errors are concentrated in the corners where the neutrons are reflected on two surfaces. In Fig. 3-4, we report the pecent errors for the z-planes 1 and 8 respectively. In Table 2 we show the CPU time spend by the isotropic and anisotropic solutions. The convergence is reached at the same number of iterations for both solutions.

5. Conclusion

The extension of the characteristics solver to include the linearly anisotropic treatment of the scattering sources, in 3D geometries, has been presented. The results, comparing the isotropic and anisotropic fluxes, show that neglecting the anisotropic effects in scattering sources may induce significant errors on flux calculation especially on the regions near the reflected boundaries.

Acknowledgements

This work has been carried out partly with the help of grants from the Natural Science and Engineering Research Council of Canada.

References

1) R. Roy, ”Anisotropic Scattering for Integral Transport Codes. Part2: Cyclic Tracking and its Application to XY Lattices”, Ann. Nucl. Energy. **18**, pp. 511-524 (1991).
2) J. L. Vujic and W. R. Martin, ”Two-Dimensional Collision Probability Algorithm with Anisotropic Scattering for Vector and Parallel Processing”, Proc. Of PHYSOR-90, Marseille, France, April 23-27, (1990).
3) R. Roy, ”Anisotropic Scattering for Integral Transport Codes. Part1: Slab Assemblies”, Ann. Nucl. Energy. **17**, pp. 379-388 (1990).
4) R. Roy, ”The Cyclic Characteristics Method with Anisotropic Scattering”, Proc. Conf. ANS-MathComp'99 , Madrid (1999).
5) T. Postma and J. Vujic, ”The Method of Characteristics in General Geometry with Anisotropic Scattering”, M&C Conference, Madrid, (1999).
6) M. Dahmani, G. J. Wu, R. Roy and J. Koclas, ”Development and Parallelization of the Three-Dimensional Characteristics Solver MCI of DRAGON”, Proc. PHYSOR 2002, Seoul, Korea, October 7-10, (2002).
7) G. Marleau, A Hebert and R. Roy, ”A User's Guide for DRAGON”, Technical Report IGE-174 Rev.3., École Polytechnique de Montréal, December (1997).
Available at: http://www2.polymtl.ca/nucl
8) J. R. Askew, ”A Characteristics Formulation of the Neutron Transport Equation in Complicated Geometries”, AEEW-M 1108 (1972).
9) B. Carlson, ”Table of Equal Weight Quadrature EQ_N Over the Unit Sphere”, Technical Report LA-4734, Los Alamos National Laboratory, (1971).

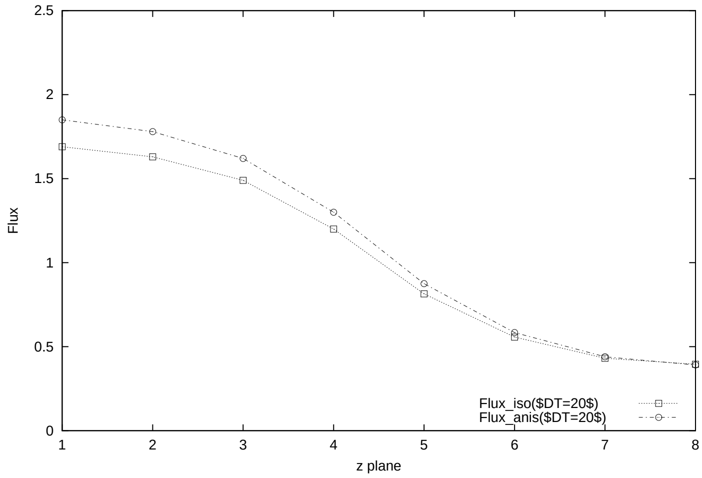

Figure 1: Isotropic and anisotropic flux for $(x = 0.25cm; y = 0.25cm)$

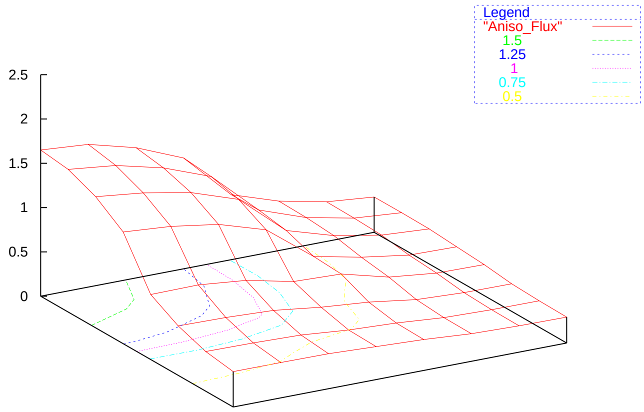

Figure 2: The Anisotropic scalar flux in plane $z = 1$ for $(8 \times 8 \times 8)$ mesh

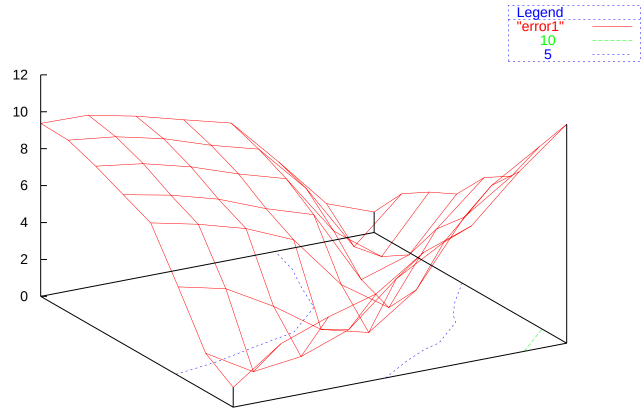

Figure 3: Percent error per region in plane $z = 1$ ($8 \times 8 \times 8$ mesh)

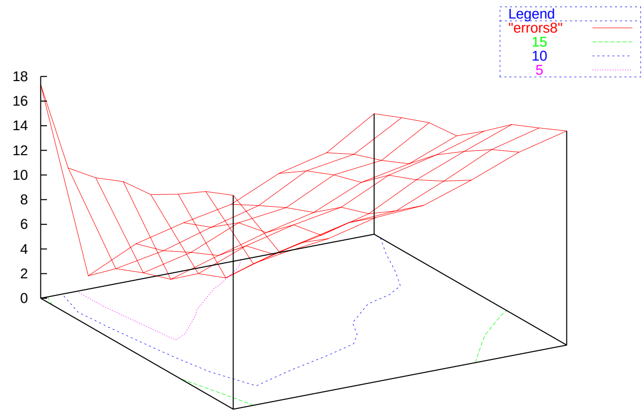

Figure 4: Percent error per region in plane $z = 8$ ($8 \times 8 \times 8$ mesh)